Room Temperature Sub-Micron Magnetic Imaging by Scanning Hall Probe Microscopy

Jpn. J. Appl. Phys. Vol. 40 (2001) pp. 4321–4324
Part 1, No. 6B, June 2001

Room Temperature Sub-Micron Magnetic Imaging by Scanning Hall Probe Microscopy

Adarsh SANDHU*, Hiroshi MASUDA[1], Ahmet ORAL[2] and Simon J. BENDING[3]

Department of Electrical Engineering, Tokai University, 1117 Kitakaname, Hiratsuka 259-1292, Japan
[1]*Toei Kogyo Ltd., 8-13-1 Tadao, Machida, 194-0035, Japan*
[2]*Department of Physics, Bilkent University, 06533 Ankara, Turkey*
[3]*Department of Physics, University of Bath, BA2 7AY, UK*

(Received January 15, 2001; accepted for publication March 19, 2001)

An ultra-high sensitive room temperature scanning Hall probe microscope (RT-SHPM) system incorporating a GaAs/AlGaAs micro-Hall probe was used for the direct magnetic imaging of localized magnetic field fluctuations in very close proximity to the surface of ferromagnetic materials. The active area, Hall coefficient and field sensitivity of the Hall probe were $0.8\,\mu\text{m}\times0.8\,\mu\text{m}$, $0.3\,\Omega$/G and $0.04\,\text{G}/\sqrt{\text{Hz}}$, respectively. The use of a semiconducting Hall probe sensor enabled measurements in the presence of externally applied magnetic fields. Samples studied included magnetic recording media, demagnetized strontium ferrite permanent magnets, and low coercivity perpendicular garnet thin films. The RT-SHPM offers a simple means for quantitatively monitoring sub-micron magnetic domain structures at room temperature.

KEYWORDS: Hall probe sensor, scanning Hall probe microscopy, magnetic recording media, garnets, magnetic imaging, magnetic domains

Methods for monitoring magnetic domains include semiconductor Hall bar sensors,[1–5] magnetic force microscopy (MFM),[6] scanning SQUID technology,[7] magneto-optical microscop[8] and Bitter patterns.[9] We have previously reported on the main features of a new room temperature scanning Hall probe microscope (RT-SHPM) that we developed for the quantitative and non-invasive magnetic imaging of localized surface magnetic fluctuations.[10]

In this paper, we describe recent results obtained by using the RT-SHPM that include: (i) imaging of hard disk test samples; (ii) the height dependence of stray magnetic fields from 'magnetic transitions' of written floppy disks; (iii) extremely rapid measurements of hysterical changes of magnetic bubble domains in uniaxial garnet films due to perpendicular external magnetic bias fields.

The RT-SHPM system was specifically designed for operation at room temperature for scans up to $50\times50\,\mu\text{m}^2$. The main components are shown in Fig. 1. The Hall probe sensor (HP) was fabricated using a GaAs/AlGaAs heterostructure grown by molecular beam epitaxy (MBE) with a two dimensional electron gas density of $2\times10^{11}\,\text{cm}^{-2}$ and mobility of $400{,}000\,\text{cm}^2$/Vs, at 4.2 K. Photolithography was used to fabricate Hall probes 13 microns away from the chip corner, which was coated with a thin gold layer to act as a scanning tunneling microscope (STM) tip. The active area of the Hall probe was $\sim0.8\,\mu\text{m}\times0.8\,\mu\text{m}$ and its Hall coefficient and field sensitivity were $\sim0.3\,\Omega$/G and $0.04\,\text{G}/\sqrt{\text{Hz}}$, respectively. The STM tip was not coupled to the Hall bar thus reducing noise during measurement.

The GaAs/AlGaAs heterostructure micro-Hall probe sensor was mounted onto a piezoelectric scanning tube (PZT) at a tilt angle of 1.5° with respect to the sample surface and the STM tip used for precise vertical positioning of the HP. The procedure for magnetic imaging consists of initially using a combination of high-resolution stepper motors (coarse) and the PZT (fine) to position the HP in close proximity to the sample surface until a tunnel current is detected. After a stable tunnel current is established, the HP is scanned over the surface while simultaneously monitoring changes in Hall voltage that are proportional to fluctuations of the perpendicular component of the magnetic field emanating from the surface.

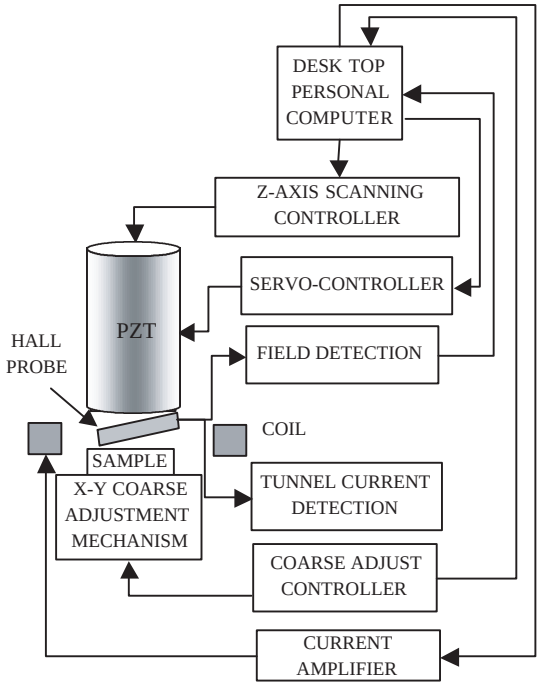

Fig. 1. Main components of room temperature scanning Hall probe microscope system.

Three measurement modes can be used for data acquisition: (a) the FAST-SHPM mode, where only the HP output is monitored and displayed during measurement; (b) the STM/SHPM mode, where the STM tip tunnel current and HP signal are both monitored, for the simultaneous measurement of surface topography and corresponding magnetic field fluctuations; (c) REAL-TIME SHPM mode, where the entire measurement is completed before the magnetic image is displayed, for ultra-high speed scans of up to 1 frame per second.

The raw two-dimensional gray-scale image data of RT-SHPM scans is stored in either a bit-map or ASCII format. For 3D visualization and animation of the raw data, we developed a unique set of program routines using the Interactive Data Language.[11]

Figures 2(a) and 2(b) show the SHPM/STM mode mag-

*E-mail address: sandhu@keyaki.cc.u-tokai.ac.jp

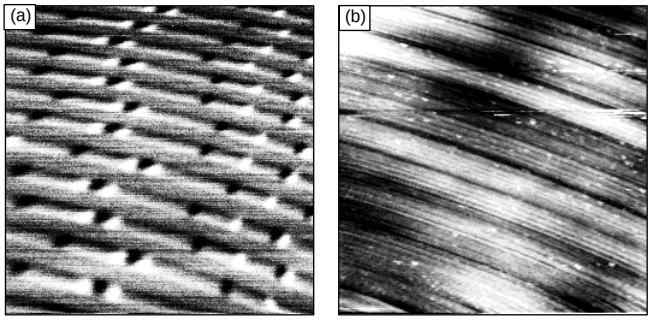

Fig. 2. (a) SHPM/STM magnetic image of a magnetic hard disk test sample ($50\,\mu\text{m} \times 50\,\mu\text{m}$). (b) STM tip topographic image of the same hard disk test sample.

netic image and corresponding simultaneous STM topographic image of a hard disk test sample ($50\,\mu\text{m} \times 50\,\mu\text{m}$). The black and white regions represent stray fields of 'magnetic transitions' with magnetizations into and out of the plane of the paper where fields vary between ± 80 Gauss from black to white. The vertical scale of the topographic image is 90 nm from black to white. The magnetic image shows the written tracks as having transitions with a range of spacings and patterns. The topographic image, on the other hand, is completely different from its magnetic counterpart and shows concentric rings that were produced during the polishing stage of the disk sample. The marked difference between the magnetic and topographic images demonstrates the ability of the RT-SHPM to distinguish magnetic data from that due to surface undulations.

Figure 3 shows a typical $50\,\mu\text{m} \times 50\,\mu\text{m}$ STM/SHPM mode image of a 100 MB 'zip' disk media and corresponding field variation along one of its tracks. The black and white regions correspond to surface fields ranging between ± 58 Gauss. It is interesting to note the non-uniformity of the field variation of the transitions along the track.

Figure 4(a) is a $25\,\mu\text{m} \times 25\,\mu\text{m}$ image of a written-track on a commercially available 1.4 MB floppy disk obtained using the STM/SHPM mode. Written transitions spaced approximately $2\,\mu\text{m}$ apart can be clearly seen with field variations between ± 120 Gauss as shown in Fig. 4(b). The 'noisy' area to the right hand side of the transitions is the unwritten region between tracks. Figure 4(c) shows the variation of magnetic field at distances ranging between 0.28 and $1.5\,\mu\text{m}$ above the

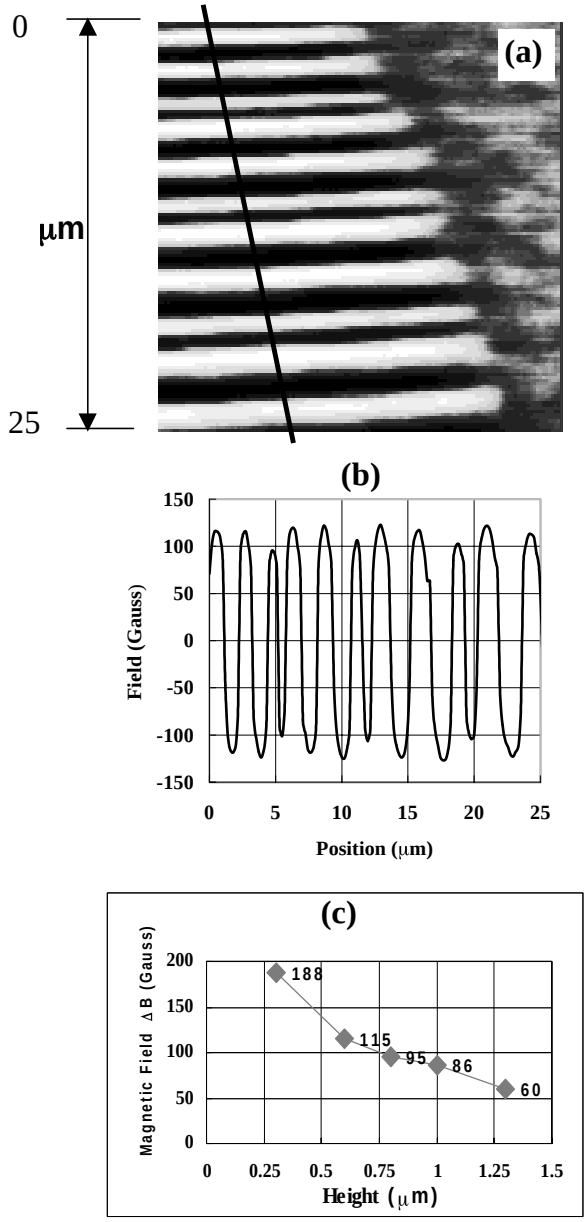

Fig. 4. (a) $25\,\mu\text{m} \times 25\,\mu\text{m}$ RT-SHPM magnetic image of a written track on a floppy disk. (b) Magnetic field variation along the long line shown. (c) Variation of magnetic fields at distances between 0.28 and $1.5\,\mu\text{m}$ above the floppy disk surface for $25\,\mu\text{m} \times 25\,\mu\text{m}$ area scans.

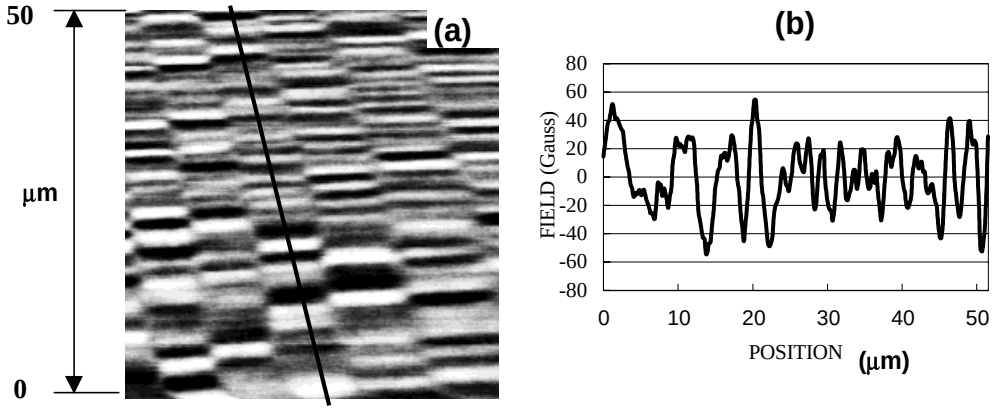

Fig. 3. (a) STM/SHPM mode image of written tracks on a 100 MB ZIP disk media. (b) Variation of magnetic field along line.

floppy disk surface for 25 μm × 25 μm area scans.

Figure 5 shows representative 25 μm×25 μm REAL-TIME SHPM mode images of a 5.5 μm thick bismuth substituted iron garnet uniaxial thin film under external perpendicular bias fields as indicated. Each image was measured in less than 10 seconds at each of the external bias fields. The images clearly show the initial hexagonal magnetic bubble lattice to persist up to a critical field of 1131 Oe. Reducing the bias field is seen to lead to the formation of stripe domains, demonstrating configurational hysteresis as previously observed using the Faraday effect.[12] Our RT-SHPM measurements showed the magnetic fields due to domain patterns to vary between ±59 G during the cycling of the external bias field between ±1500 Oe. These results showing bubble collapse and subsequent formation of stripe domains, could be used for characterizing uniaxial thin films and determining parameters such as wall energy and saturation magnetization without the need for magnetometer measurements.[13]

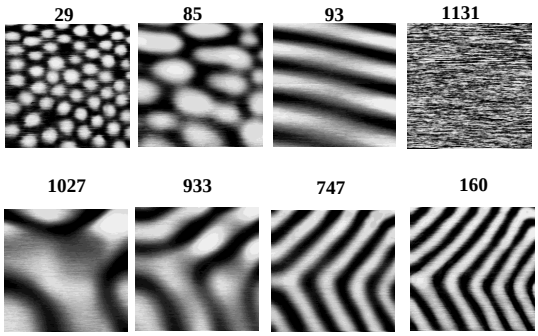

Fig. 5. Representative 25 μm × 25 μm REAL-TIME SHPM mode images of a 5.5 μm thick bismuth substituted iron garnet uniaxial thin film under external perpendicular bias fields (Oe) as indicated.

Figure 6 shows a 50 μm×50 μm SHPM image of a 360 μm thick Bi substituted iron garnet thin film. The image resembles 'fujitsubo' (barnacles). The image reveals a very complicated spatial field distribution that cannot be observed using conventional optical techniques often used for characterizing garnets.

Figures 7(a) and 7(b) show the RT-SHPM images of a demagnetized Sr ferrite magnet without and with (1760 Oe) an external perpendicular field, respectively. Domain structures are clearly imaged and are seen to increase in size on application of the external field. Further RT-SHPM analysis of domain wall movement in ferrite and other permanent mag-

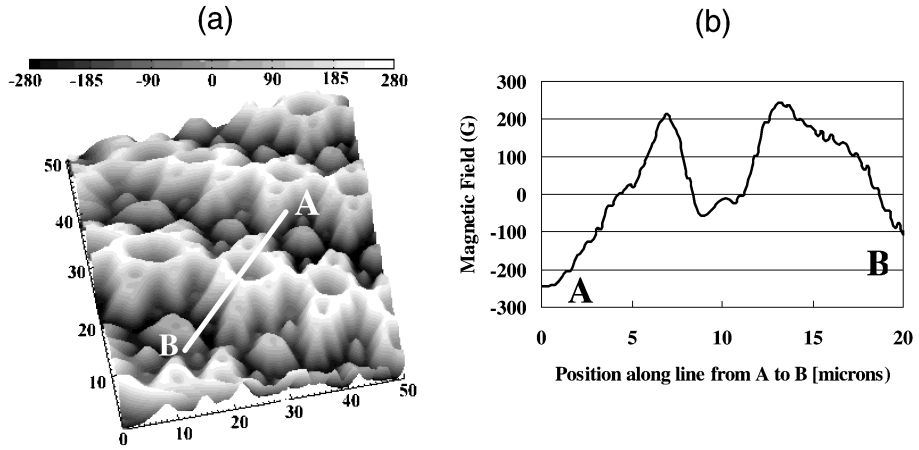

Fig. 6. (a) 'Fujitsubo-like' image of a 360 μm thick Bi substituted iron garnet uniaxial film. (b) Variation of magnetic field across line A-B

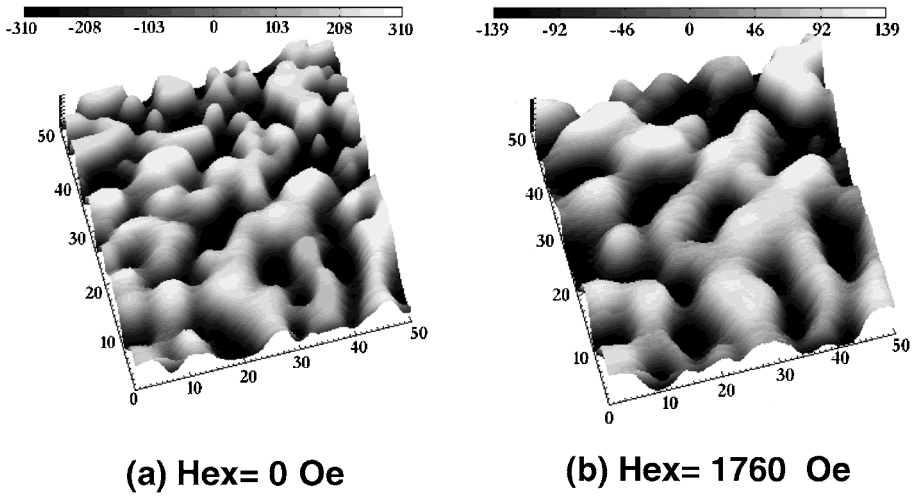

Fig. 7. (a) RT-SHPM image of a 400 μm thick demagnetized Sr ferrite permanent magnet. (b) RT-SHPM image of the same magnet placed an external perpendicular field of 1760 Oe.

nets is being carried out for a deeper understanding of the relationship between domain size and coercivity and saturation magnetization for the development of high performance permanent magnets.[14)]

A new versatile room temperature scanning Hall probe microscope system was used for the quantitative magnetic imaging of hard disk test samples, floppy disks, uniaxial thin film garnets and demagnetized strontium ferrite magnets. The system will be a valuable tool in the development of information storage media, permanent magnets and new technology related to semiconductor/ferromagnetic hybrid structures being studied for the next generation of magneto-electronic devices.

1) H. T. Coffey: Cryogenics **7** (1965) 73.
2) M. Tinkham: J. Low Temp. Phys. **5** (1971) 5465.
3) M. A. Itzler, J. A. Simmons and P. M. Chaikin: Bull. Am. Phys. Soc. **36** (1991) 724.
4) A. M. Chang, H. D. Hallen, L. Harriott, H. F. Hess, H. L. Kao, J. Kwo, R. E. Miller, R. Wolfe, J. van der Ziel and T. Y. Chang: Appl. Phys. Lett. **61** (1992) 1974.
5) Oral, S. J. Bending and M. Henini: J. Vac. Sci. & Technol. B **14** (1996) 1202.
6) U. Hartmann: J. Vac. Sci. & Technol. **A8** (1990) 411.
7) C. C. Tsuei, J. R. Kirtley, C. C. Chi, L. S. Yu-Jahnes, A. Gupta, T. Shaw, J. Z. Sun and M. B. Ketchen: Phys. Rev. Lett. **73** (1994) 593.
8) J. M. Florczak and E. D. Dahlberg: J. Appl. Phys. **67** (1990) 7520.
9) G. C. Rauch, R. F. Krause, C. P. Izzo, K. Foster and W. O. Barlett: J. Appl. Phys. **55** (1984) 2145.
10) A. Sandhu, H. Masuda, A. Oral and S. J. Bending: Proc. 8th Int. Conf. Ferrites, Kyoto, Sept. 18-21, 2000.
11) Research Systems, Inc., 4990 Pearl East Circle, Boulder, USA.
12) K. L. Babcock and R. M. Westervelt: Phys. Rev. **A 40** (1989) 2022.
13) T. G. W. Blake, C. C. Shur, Y. T and E. D. Torre: IEEE Trans. Magn. **18** (1982) 985.
14) H. R. Kirchmayr: J. Phys. **D29** (1996) 2763.